analytical chemistry

Article

pubs.acs.org/ac

Hybrid Capillary/Microfluidic System for Comprehensive Online Liquid Chromatography-Capillary Electrophoresis-Electrospray Ionization-Mass Spectrometry

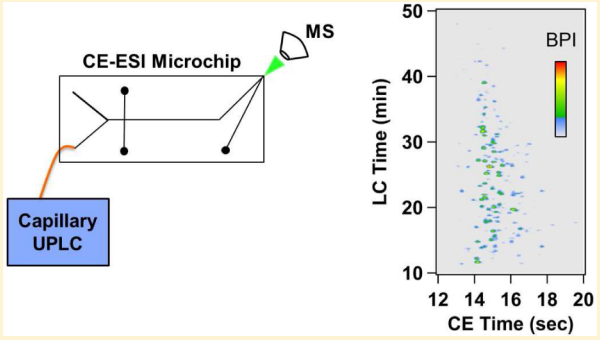
J. Scott Mellors,[†] William A. Black,[†] Andrew G. Chambers,[†] Jason A. Starkey,[∥] Nathan A. Lacher,[∥] and J. Michael Ramsey*[,†,‡,§]

[†]Department of Chemistry, [‡]Department of Biomedical Engineering, and [§]Carolina Center for Genome Sciences, University of North Carolina, Chapel Hill, North Carolina 27599, United States

[∥]Pfizer Biotherapuetics R&D, Pfizer Inc., Chesterfield, Missouri 63017, United States

Supporting Information

ABSTRACT: A hybrid multidimensional separation system was made by coupling capillary liquid chromatography (LC) to a microfluidic device. The microfluidic device integrated flow splitting, capillary electrophoresis (CE), electroosmotic pumping, and electrospray ionization (ESI) emitter functional elements. The system was used with a time-of-flight mass spectrometer for comprehensive online LC-CE-MS of proteolytic digests. Analysis of a complex mixture of peptides yielded a peak capacity of approximately 1400 in 50 min. Three replicate runs demonstrated mean reproducibility for LC retention and CE migration times of 0.32% and 0.75% relative standard deviation (RSD), respectively. The same LC-CE-MS method was also used to characterize the N-linked glycosylation of a monoclonal antibody. Glycopeptides from two different N-linked glycosylation sites were separated from all other tryptic peptides and identified using MS data. The relative amounts of each glycoform and total site occupancy were quantified using LC-CE-MS data.



Microfluidic devices have advantages over conventional hardware for integration of numerous functional elements and rapid, precise manipulation of small volumes.[1] These properties make them an ideal platform for multidimensional separations as demonstrated by several microfluidic systems utilizing different combinations of separation modes that have been reported.[2−9] Many of the reported methods were capable of rapid and powerful separations, but without mass spectrometry (MS) detection they had limited practical utility.

We recently developed a method for coupling microfluidic devices to MS detection via monolithic integration of an electrospray ionization (ESI) emitter.[10] Highly stable and sensitive ESI-MS was realized without broadening the narrow, low volume analyte bands produced by microfluidic separations. Using this ESI interface we created a monolithic multidimensional separation system with liquid chromatography (LC), capillary electrophoresis (CE), and ESI integrated on a single microfluidic device.[11] Used for online LC-CE-MS, this system yielded far better performance than previously reported capillary-based systems.[12−14]

Although the fully integrated LC-CE-MS system clearly demonstrated the advantages of microfluidics for multidimensional separations, we found that integration of the LC column within the microfluidic device limited the performance of the system. The fittings that connected the device to an external pressure source could not reliably hold more than 200 bar. This limited the minimum stationary phase particle diameter and column length, and therefore the efficiency of the LC column. It also necessitated manually packing each device with stationary phase particles. This increased fabrication time and could decrease device to device reproducibility. Moving the LC column off of the device and using a conventional capillary LC column alleviated these problems. The potential drawback to such a hybrid system would be dead volume band-broadening in the capillary to microchip connection. The same capillary to microchip fittings described in our previous work[11] had sufficiently low dead volume (less than 20 nL) that band-broadening through the connection was not a limiting factor for the hybrid approach described below.

Previous demonstrations of LC-CE and LC-CE-MS have used peptide mixtures to characterize system performance.[6,11−23] It has been suggested that the two-dimensional image plot from an LC-CE separation of tryptic peptides could be used as a protein fingerprint,[12,15,16,18,21] but a real world application of this technology has not yet been demonstrated.

Received: January 20, 2013
Accepted: March 11, 2013
Published: March 11, 2013

 © 2013 American Chemical Society

One application that might benefit from the unique capabilities of LC-CE-MS is the mapping of post-translational modifications of complex biotherapeutics. For this work, we chose to characterize the N-linked glycosylation of a monoclonal antibody by glycopeptide mapping.[24,25] It has been shown that one-dimensional LC-MS can be used for this application. Specifically, LC-MS/MS of tryptic digests can identify multiple glycosylation sites, determine the percentage of site occupancy, and quantify the relative abundance of each glycoform at multiple sites.[26,27] LC-CE-MS can improve this method by two ways: first, by separating the glycopeptides from all other sample components in less time and with less method development; and second, by improving glycopeptide identification confidence by using LC retention and CE migration times to confirm identity. In this work we evaluate the peak capacity and reproducibility of the hybrid LC-CE-MS system by separating a complex mixture of tryptic peptides. We then demonstrate an application of this system by mapping the N-linked glycosylation of a monoclonal antibody with two N-linked glycosylation sites.

EXPERIMENTAL SECTION

Reagents and Materials. Acetonitrile (Optima LC/MS), 2-propanol (Optima LC/MS), formic acid, and potassium hydroxide were obtained from Fisher Chemical (Fairlawn, NJ). Water was purified by a Nanopure system fitted with a 0.2 μm filter (Barnstead International, Dubuque, IA). 3-Aminopropyltriethoxysilane, trichloro(1H,1H,2H,2H-perfluorooctyl)silane, and protein standards (bovine serum albumin, ovalbumin, enolase, and alcohol dehydrogenase) were acquired from Sigma Chemical Co. (St. Louis, MO). Sequencing grade modified trypsin was from Promega (Madison, WI).

A mixture of five trypsin digested proteins was prepared as follows: equimolar amounts of four proteins (bovine serum albumin, ovalbumin, enolase, and alcohol dehydrogenase) were denatured with guanidine hydrochloride at 60 °C. Proteins were then reduced with dithiothreitol, alkylated with iodoacetamide, and digested with trypsin for 4 h at 37 °C. After digestion, peptides were collected by solid phase extraction on an Oasis HLB cartridge (Waters Corp.) A phosphorylase B tryptic digestion standard (massPrep, Waters Corp.; Milford, MA) was added as an internal standard. The mixture was then diluted with 3% acetonitrile, 0.1% formic acid to an approximate concentration of 500 nM for the four in-house digested proteins and 200 nM for phosphorylase B.

A tryptic digest of an immunoglobulin G2 (IgG2) monoclonal antibody was provided by Pfizer Inc. using the following procedure: The IgG protein sample was diluted to 4.0 mg/mL with 20 mM sodium acetate (pH 5.5). Trypsin was activated and diluted according to the manufacturer's recommendations. A volume of 100 μL of diluted protein solution was added to 50 μL of acetonitrile and 10 μL of 500 mM Tris buffer (pH 8.5) and mixed well. The mixture was transferred to a vial containing 20 μg of resuspended trypsin and incubated for 24 h at 37 °C. At the end of incubation, 10 μL of 1 N HCl was added to the mixture and mixed well to quench the digestion. Samples were diluted to a concentration of approximately 0.1 mg/mL with 3% acetonitrile, 0.1% formic acid before analysis by LC-CE-MS.

Microchip Design and Fabrication. The microfluidic device (shown schematically in Figure 1) incorporated five distinct functional elements: a pressure-driven flow splitter, a CE injection cross, a CE separation channel, an electroosmotic pump, and an ESI emitter. The addition of the flow splitter is the only fundamental difference between this design and our previously described CE-ESI devices.[10] The flow splitter was necessary to decouple the LC and CE flow rates, so both dimensions could be optimized. For this LC-CE-MS system the channel dimensions were designed so that $^1/_3$ of the pressure-driven LC eluent would be directed to the injection cross. All channels were etched to a depth of 10 μm. Channel lengths were LC inlet before split, 13 mm; LC inlet after split, 4 mm; split flow, 13 mm; buffer, 8 mm; waste, 8 mm; CE channel, 91 mm; EO pump, 22 mm. The short channel segment between the EO pump intersection and the ESI corner was less than 0.2 mm long (not visible in Figure 1). Straight channel segments were 95 μm wide at full width except for the split flow channel, which was broadened to 295 μm to decrease the hydrodynamic resistance and thus control the pressure driven flow split. The serpentine turns in the CE channel were asymmetrically tapered down to a full width of 30 μm to minimize band-broadening, as previously described.[10,28]

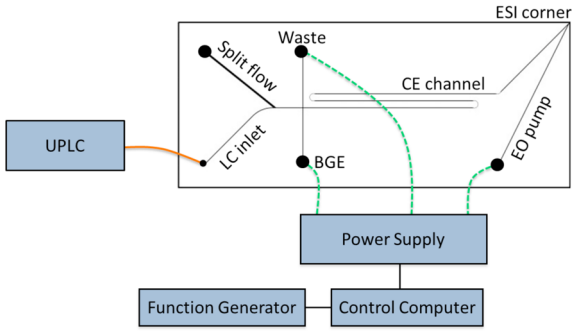


Figure 1. Schematic of the hybrid capillary LC microchip CE-ESI experimental setup. The orange line represents a transfer capillary connecting the LC column to the microfluidic device. The dashed green lines represent electrical connections between the high voltage power supply and the microfluidic reservoirs. The device was positioned with the ESI corner approximately 5 mm from the mass spectrometer inlet. Channel dimensions are given in the Experimental Section.

The microfluidic device was fabricated by standard photolithography and wet chemical etching methods as described previously.[10,29] The device was fabricated from 0.15 mm thick borosilicate glass substrates (Thermo Fisher Scientific., Portsmouth, NH), coated with chrome and photoresist by Telic Co. (Valencia, CA). Access ports for the LC inlet and fluid reservoirs were drilled through the etched substrate using a Microblaster powder blaster (Comco Inc., Burbank, CA) fitted with a 0.38 mm i.d. nozzle. After bonding the etched substrate to a cover plate, the electrospray tip was machined by dicing the corner of the device with a precision saw (Dicing Technology, San Jose, CA) as previously reported.[10] To protect the device from mechanical damage, the device was attached to 0.9 mm thick glass with transparent UV epoxy (Norland Products Inc., Cranbury, NJ). Glass cylinder solvent reservoirs (200 μL capacity) were attached to the device with a chemical resistant epoxy (Loctite E-120HP Hysol, Henkel Corp., Rocky Hill, CT).

Surface Modification. All internal and external surfaces of the microfluidic device were coated with aminopropyltriethoxysilane (APTES) using a gas phase deposition method. The covalently bound aminopropyl groups gave these microchannels a positive surface charge, providing anodic electroosmotic flow (EOF). A full description of this coating method

dx.doi.org/10.1021/ac400205a | Anal. Chem. 2013, 85, 4100−4106

along with a detailed characterization of the surface is currently in production. Briefly, microfluidic channels were prepared by flushing for 15 min with a mixture of 1 N potassium hydroxide in 80% by volume 2-propanol (KOH/IPA). Flushing was accomplished by attaching a vacuum line to the ESI corner of the device. The channels were thoroughly rinsed with deionized water and dried. The microchip was then placed in the chamber of a LabKote vapor deposition system (Yield Engineering Systems, Livermore, CA), heated to 130 °C. After purging the chamber with nitrogen, the chamber was evacuated to a base pressure of 0.1 Torr. APTES (0.3 mL) was then injected into the chamber, raising the chamber pressure to ∼1.5 Torr. After a 30 min exposure, the pressure was cycled and another injection was performed. A total of 3, 0.3 mL reagent injections and 3, 30 min exposures were performed. Finally the chamber was purged with nitrogen to remove excess reagent vapor and the microfluidic device was removed. After silanization, the EO pump channel was selectively flushed with KOH/IPA for 2 h to remove the aminopropyl silane coating. The other channels were filled with 2-propanol during this process. The device was then flushed thoroughly with deionized water and the surface of the electrospray tip was coated with trichloro (perfluorooctyl) silane to prevent wetting and droplet formation as previously described.[11,30] The same microfluidic device was used over a 4 week period without further surface treatment to collect all data presented in this manuscript.

Liquid Chromatography. A nanoAcquity UPLC system (Waters Corp., Milford, MA) was used for the LC separations. The analytical column (Waters part number 186003543) was 150 mm long, 75 μm i.d., packed with 1.7 μm BEH130 C18 particles. The trapping column (Waters part number 186003514) was 20 mm long, 180 μm i.d. packed with 5 μm symmetry C18 particles. Mobile phase A was 0.5% acetonitrile with 0.1% formic acid, while mobile phase B was 99.5% acetonitrile with 0.1% formic acid. The mobile phases were degassed by sonication under vacuum before use. During the 2 min trapping step, the mobile phase composition was 1% B with a flow rate of 10 μL/min. The injection volume for all data presented here was 2 μL. A 60 min gradient from 7% to 40% B at a flow rate of 500 nL/min and an analytical column temperature of 35 °C was used for all separations presented. For LC-MS, the transfer capillary leading from the analytical column was connected to a 10 μm i.d. Picotip emitter (New Objective, Woburn, MA) via a Universal Nanoflow Sprayer interface (Waters Corp., Milford, MA). For LC-CE-MS, the transfer capillary leading from the analytical column was connected to the microfluidic device using a previously described custom fitting.[11]

Microchip Operation. The electrokinetically gated CE injection method has been previously described.[11] Electric potentials were applied to the fluid reservoirs from a custom built power supply which was computer controlled using an in-house written LabVIEW program (National Instruments, Austin, TX). Appropriate safety precautions should always be taken when working with high voltage. CE injections were performed by periodically altering the voltages to allow small plugs of the LC eluent into the CE separation channel. When the CE injection gate was closed the voltages applied to the reservoirs (illustrated in Figure 1) were BGE, −6 kV; waste, −3 kV; EO pump, +4.6 kV. In this state, flow from the BGE reservoir flowed down the CE separation channel and gated the LC eluent to waste. When the CE injection gate was open, the voltages applied to the reservoirs were BGE, −4.75 kV; waste, −4.25 kV; EO pump, +4.6 kV. The field strength in the separation channel was the same for both voltage states, so overlapping injections[18] could be used without perturbing the previous separation. Injections lasting 0.1 s were performed every 10 s. The CE injection cycle was initiated before the sample was injected onto the LC column and continued through the duration of the run. To ensure proper timing over long periods of time, an external function generator (Agilent Technologies model 33220A) was used to trigger the CE injections. The background electrolyte (BGE) for the CE separations was 50% acetonitrile, 0.1% formic acid. The voltages applied to the microfluidic reservoirs provided an electrophoretic separation field of approximately 800 V/cm and an ESI voltage of +3 kV. The difference in EOF between the APTES coated separation channel and the uncoated EO pump channel caused fluid to be pumped out of the ESI orifice at approximately 400 nL/min (350 nL/min anodic flow from the separation channel plus 50 nL/min cathodic flow from the EO pump channel).

Mass Spectrometry. An LCT Premier orthogonal acceleration time-of-flight (oa-TOF) mass spectrometer was used (Waters Corp.). Data were acquired in V mode from 300 to 1600 m/z at a rate of 10 Hz (90 ms per summed scan with an interscan delay of 10 ms). The microchip was held on an x,y,z translational stage and positioned with the electrospray corner approximately 5 mm from the inlet of the mass spectrometer as previously described.[10] The MassLynx data collection software was triggered to begin saving at the first CE injection after the LC injection. Data collection continued as a single file for the duration of the LC-CE-MS run.

Data Processing. LC-CE-MS data were processed into 2D image plots as described previously.[11] Briefly, data were exported from Masslynx as two columns (LC run time and ion count). A Labview program was used to generate a third data column representing CE migration time. The program worked by performing iterative subtraction of the time between CE injections (10 s) from the original LC run time data until all data points had a value between 0 and 10 s. The actual dead time of the CE runs was about 2 s longer than the CE injection period, so the original run time data points were all shifted by −2 s to properly center the time window. Because of this shift and the use of overlapping injections, this method produced CE migration time values that were 12 s lower than the actual CE migration times. These 12 s were added back when the data were plotted. The three data columns (CE migration time, LC run time, and ion count) were loaded into an open source imaging program (Image J, U.S. National Institutes of Health, available at http://rsb.info.nih.gov/ij) with an available plugin (XYZ2DEM importer). The resulting image was loaded into Igor Pro (WaveMetrics, Lake Oswego, OR) for additional graphing options.

Data from the LC-CE-MS separation of the monoclonal antibody were additionally processed using BiopharmaLynx version 1.2 (Waters Corp.). We used a method designed for LC-MS peptide mapping, modified to search for a peak width of just 0.01 min with an MS threshold of 100 counts. The amino acid sequence and disulfide linkages of this molecule were provided by Pfizer Inc. The modifications search included the common N-linked glycosylations illustrated in Figure 2. BiopharmaLynx was not designed to process multidimensional data, so the software processed the LC-CE-MS data as if it were LC-MS data. It identified each LC-CE-MS peak as a separate component, assigning the same molecular mass and peptide

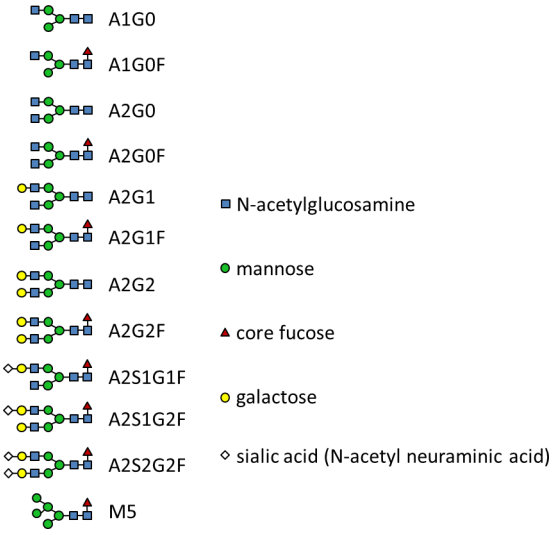


Figure 2. Structures of common N-linked glycans examined in this manuscript.

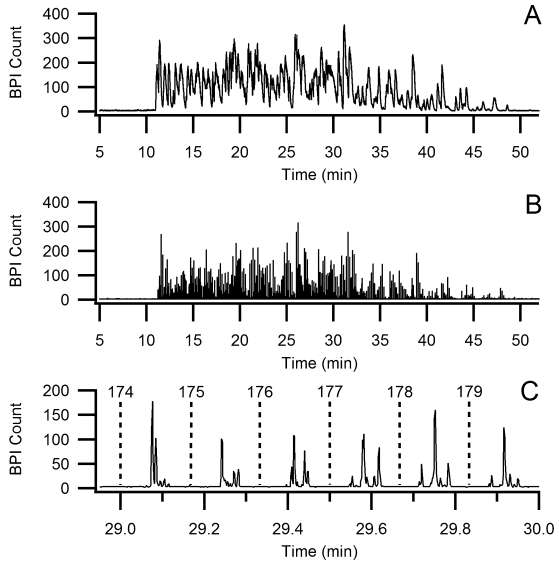


Figure 3. LC-MS chromatogram (A) and LC-CE-MS chromato-electropherogram (B,C) for the analysis of a five-protein tryptic digest mixture. All LC conditions and MS acquisition settings were identical for these two runs. The bottom plot (C) is an expanded view of a segment of the data shown in part B. The dashed lines indicate when CE injections were performed, with labels to indicate the injection number.

identification to multiple peaks. In other words the peak matching algorithm did not use CE migration time data to help it identify peaks, but it was also not confused by the presence of multiple narrow peaks with the same molecular mass. The relative abundance of each glycoform was calculated by a manual summation of the total MS intensity for all peaks assigned to each N-linked glycopeptide. The LC retention and CE migration times were found by generating a separate 2D image plot using extracted ion chromato-electropherograms for each identified N-linked glycopeptide.

RESULTS AND DISCUSSION

Evaluation of System Performance. The LC-CE-MS system was evaluated for total peak capacity and reproducibility using the five-protein tryptic digest. For comparison this sample was separated by LC-MS and LC-CE-MS using identical LC conditions. The base peak ion count (BPI) chromatogram for the LC-MS run is displayed along with the BPI chromato-electropherogram for an LC-CE-MS run in Figure 3. The individual peaks of the LC-CE-MS run are too brief to see in Figure 3B, so a 1-min wide section of this run is displayed in Figure 3C. The peaks from sequential CE runs can be clearly seen, spaced by the 10 s period of the CE injections. Dashed lines indicate the times at which the labeled CE injection number occurred. Because overlapping injections were used, the peaks are offset by one injection period. In other words, the first group of CE peaks visible in Figure 3B came from injection number 173, and the peaks from injection number 179 are not visible in this figure. Figure 4 shows a two-dimensional image plot generated from the same data displayed in Figure 3B. This plot gives a better representation of the power of this multidimensional separation. In this plot the color of the spots corresponds to the intensity of the base peak ion count. The position of each spot corresponds to its LC retention and CE migration times. Spot position therefore indicates the hydrophobicity and electrophoretic mobility of the detected compound.

Comparison of extracted ion chromatograms for the LC-MS and LC-CE-MS separations of the five-protein tryptic digest confirmed that the peptide bands had similar temporal widths in both runs (Figure S1 in the Supporting Information).

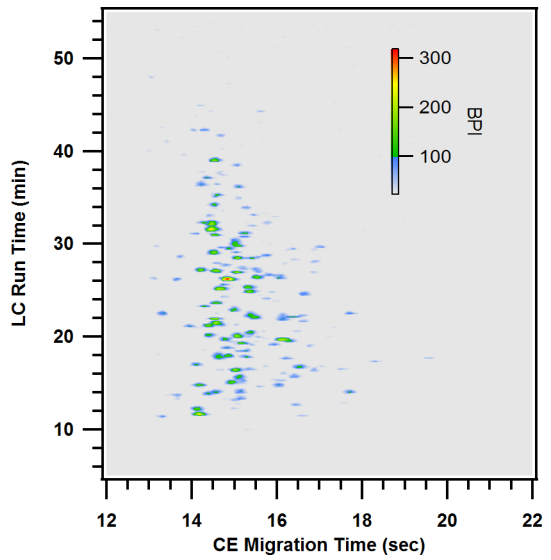


Figure 4. Image plot for the LC-CE-MS separation of a five-protein tryptic digest mixture. This plot was generated from the same data shown in figure 3B.

Therefore, the LC-MS separation of the five protein tryptic digest was used to estimate peak capacity for the LC dimension of the LC-CE-MS run. The LC-MS BPI chromatogram contained too many unresolved peaks to accurately measure peak widths, so an extracted ion chromatogram from a small m/z range (700–710) was used. This chromatogram was processed with an open source software program (Peak Finder, available at http://omics.pnl.gov/software) to estimate the median 4σ peak width. A total of 30 peaks were fit, yielding a median peak width of 16.5 s. To calculate peak capacity, the full width of the LC separation window was determined from the LC-CE-MS data by subtracting the run time of the first

dx.doi.org/10.1021/ac400205a | Anal. Chem. 2013, 85, 4100–4106

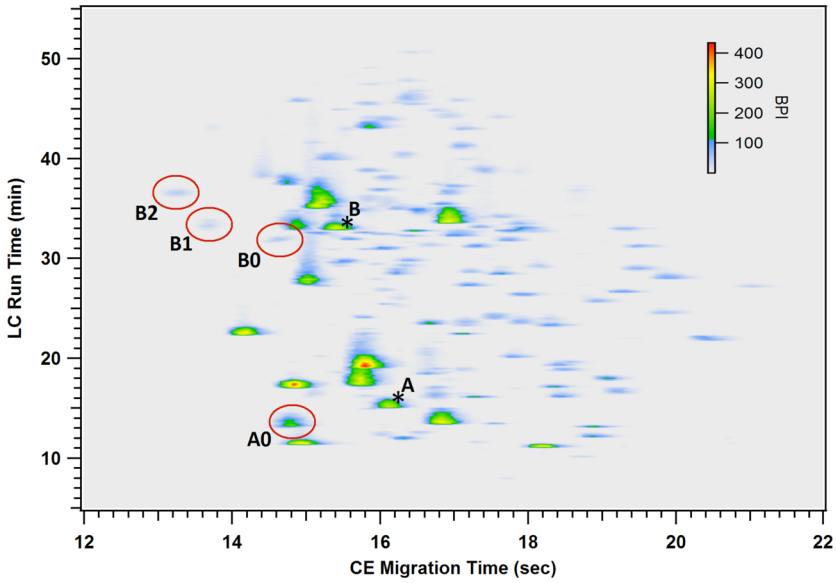


Figure 5. Image plot for the LC-CE-MS separation of a digested IgG2 containing two N-linked glycosylation sites. The circled spots contained all of the observed N-linked glycopeptides. The spot labeled A0 contained all of the glyopeptides from the Fc domain site. Spots B0, B1, and B2 contained the glycopeptides from the Fab domain site containing 0, 1, and 2 sialic acid residues, respectively. The positions of corresponding unglycosylated peptides from each site are indicated with asterisks (*).

observed peptide peak (~11 min) from the run time of the last observed peptide peak (~49 min). Dividing the LC separation window by the 4σ peak width gave an LC peak capacity of 138. The median CE peak width was determined by processing the entire BPI chromato-electropherogram for the LC-CE-MS separation of the five-protein tryptic digest using the same software program. A total of 334 peaks above a threshold of 30 BPI were identified with a median peak width of 0.44 s. The average width of the CE separation windows was estimated by visual examination of the image plot shown in Figure 3 to be approximately 4.5 s. This average window divided by the median peak width of 0.44 s yielded an average CE dimension peak capacity of 10.2. Multiplying the estimated peak capacities of the LC and CE dimensions yielded a total LC-CE peak capacity of approximately 1400, over an order of magnitude greater than the LC-MS run with no increase in analysis time. The reproducibility of the system was measured with three replicate LC-CE-MS runs of the same five-protein tryptic digest sample (Figure S2 in the Supporting Information) performed on the same day. The spot locations of 10 randomly selected components were identified in the image plots for each replicate run. For these 3 replicate runs, the average relative standard deviations (RSD) for LC retention and CE migration times of these 10 spots were 0.32% and 0.75%, respectively.

N-linked Glycosylation Analysis of a Monoclonal Antibody. After characterizing the performance of the LC-CE-MS system, the same method described above was applied to glycosylation profiling of a monoclonal antibody. The molecule studied was an immunoglobulin G2 (IgG2) with two heavy chain N-linked glycosylation sites, one in the Fc domain and one in the Fab domain. The sample was prepared by digestion with trypsin but was not chemically modified in any other way. N-glycans were therefore attached to one of two tryptic peptides (EEQFNSTFR from the Fc domain and NTSISTAYMELSSLR from the Fab domain). Figure 5 shows the 2D image plot generated from this analysis. The spots containing all of the observed N-linked glycopeptides are circled on this plot. Unglycosylated tryptic peptides from each glycosylation site were also observed. These two spots are not visible in Figure 5 because they were of low abundance and they both coeluted with other highly abundant peptides. However, their locations, determined from extracted ion plots, are indicated by asterisks. Table 1 lists all of the observed N-linked glycopeptides along with observed masses, locations in Figure 5, intensities, and relative abundances.

A closer examination of the data displayed in Figure 5 and Table 1 indicates some important features of this separation. First we can see that all of the N-linked glycopeptides were fully resolved from other highly abundant peptides. The presence of intense spots at the same horizontal or vertical position in the plot indicates that this would not have been the case for a one-dimensional LC or CE separation. Second, we can see that the glycopeptide spots are located in predictable regions relative to each other and their corresponding aglyco peptides. Neutral glycosylations (spots A0 and B0) shifted the position relative to the aglyco peptides (spots A* and B*) to earlier LC retention and CE migration times. As expected from the greater relative change in molecular mass, the shift was greater for the smaller Fc domain peptide (A). Except for the addition of a sialic acid residue, differences in N-glycan structure had little effect on LC retention or CE migration. The addition of each sialic acid residue caused a significant shift to earlier CE migration and later LC retention. Finally, we can see significant differences in the glycosylation profiles of the two different sites. This highlights the importance of maintaining site specific information by analyzing glycosylation at the peptide level.

There are more than 100 fully resolved spots visible in Figure 5. This clearly indicates that far more information is available in this data than what we have analyzed here. To fully exploit the power of this technology we need to improve data analysis software. We were able to generate 2D image plots from our LC-CE-MS data, but we can only display a single ion count (total ion, base peak, or extracted ion counts) as the color scale in these plots. To access the wealth of MS data generated by this method we had to refer back to the linear raw data file. We were not able to sum spectra in the 2D separation space. There

dx.doi.org/10.1021/ac400205a | *Anal. Chem.* 2013, 85, 4100−4106

Table 1. N-Linked Glycopeptides Observed by LC-CE-MS Analysis of the IgG2 Tryptic Digest

N-glycan[a]	calculated mass	observed mass	spot location[b]	total intensity (counts)	% of total
Fc Domain: EEQFNSTFR					
aglyco	1 156.51	1 156.44	A	539	0.3
A1G0	2 251.91	2 251.78	A0	266	0.1
A1G0F	2 397.97	2 397.85	A0	7 613	3.8
A2G0	2 454.99	2 454.86	A0	5 479	2.7
A2G0F	2 601.05	2 600.90	A0	154 367	76.1
A2G1F	2 763.10	2 762.95	A0	25 584	12.6
A2G2F	2 925.15	2 924.98	A0	486	0.2
A2S1G1F					
A2S1G2F					
A2S2G2F					
M5	2 372.94	2 372.81	A0	8 414	4.1
sum				202 748	100.0
Fab Domain: NTSISTAYMELSSLR					
aglyco	1 671.81	1 671.73	B	2 926	4.6
A1G0					
A1G0F	2 913.27	2 913.10	B0	412	0.6
A2G0					
A2G0F	3 116.35	3 116.20	B0	12 503	19.5
A2G1F	3 278.40	3 278.24	B0	5 187	8.1
A2G2F	3 440.45	3 440.29	B0	1 928	3.0
A2S1G1F	3 569.44	3 569.31	B1	7 254	11.3
A2S1G2F	3 731.55	3 731.37	B1	13 733	21.4
A2S2G2F	4 022.64	4 022.44	B2	20 310	31.6
M5					
sum				64 253	100.0

[a]Glycan structures are defined in Figure 2. [b]Spot locations correspond to Figure 5.

are programs designed for multidimensional gas chromatography (GC × GC)-MS (e.g., ChromaTOF, LECO Corp., St. Joseph, MI), and LC-ion mobility-time-of-flight-MS (e.g., DriftScope, Waters Corp., Milford, MA) that can do this. Although we did not attempt to import our LC-CE-MS data into one of these programs, it should be possible. As mentioned above it should also be possible to use LC-CE spot position to help identify sample components. Peptide retention prediction has been integrated into bioinformatics software to improve identifications for one-dimensional LC-MS.[31,32] The added specificity of an additional separation dimension should greatly improve this type of correlation. Retention indices have been used for sample component identification in GC × GC, with considerable effort applied to accurately predicting retention in both dimensions.[33] Reichenbach et al. recently reported a method of peak pattern matching for two-dimensional liquid chromatography (LC × LC).[34] Their method could be applied to LC-CE-MS data for automated comparison of different samples. Because CE migration (dependent only on molecular size and charge) is simpler than chromatographic retention, correlation to chemical structure should be easier and more precise for LC-CE than for multidimensional methods that use two modes of chromatography.

CONCLUSION

A hybrid capillary LC-microfluidic CE-ESI system has been demonstrated for the LC-CE-MS analysis of digested proteins. This system yielded significant improvements in peak capacity and reproducibility compared to previous reports of LC-CE-MS.[11−14] The biggest advantage of this method may be the ability to easily convert an existing LC-MS system to a high peak capacity LC-CE-MS system. Connecting the microfluidic device to an LC column outlet is no more complicated than connecting a conventional ESI emitter; and CE separations can be performed by simple electronic control of three voltages. On chip flow splitting can accommodate a wide range of LC flow rates with minor adjustments to the microfluidic channel dimensions. The glycosylation profiling method demonstrated here provides a good example of the type of application that could benefit from this new technology. Improvements in data processing software should allow more complete mapping of complex proteins without any other changes to the method. This method should also become more powerful as mass spectrometer speed and sensitivity continue to improve.

ASSOCIATED CONTENT

Supporting Information

Additional information as noted in text. This material is available free of charge via the Internet at http://pubs.acs.org.

AUTHOR INFORMATION

Corresponding Author

*E-mail: jmramsey@unc.edu.

Notes

The authors declare no competing financial interest.

ACKNOWLEDGMENTS

Portions of this work were funded by Waters Corporation and Pfizer Incorporated. We thank Jean Pierre Alarie and Dr. Roswitha Ramsey for helpful comments during the production of this manuscript. Use of the Peak Finder software, written by Matthew Monroe, is acknowledged in the following statement. Portions of this research were supported by the NIH National Center for Research Resources (Grant RR018522) and the W.R. Wiley Environmental Molecular Science Laboratory (a national scientific user facility sponsored by the U.S. Department of Energy's Office of Biological and Environmental Research and located at Pacific Northwest National Laboratory (PNNL)). PNNL is operated by Battelle Memorial Institute for the U.S. Department of Energy under Contract DE-AC05-76RL0 1830.

REFERENCES

(1) Whitesides, G. M. *Nature* **2006**, *442*, 368−373.
(2) Chen, H.; Fan, Z. H. *Electrophoresis* **2009**, *30*, 758−765.
(3) Tia, S.; Herr, A. E. *Lab Chip* **2009**, *9*, 2524−2536.
(4) Rocklin, R. D.; Ramsey, R. S.; Ramsey, J. M. *Anal. Chem.* **2000**, *72*, 5244−5249.
(5) Gottschlich, N.; Jacobson, S. C.; Culbertson, C. T.; Ramsey, J. M. *Anal. Chem.* **2001**, *73*, 2669−2674.
(6) Yang, X. H.; Zhang, X. M.; Li, A. Z.; Zhu, S. Y.; Huang, Y. P. *Electrophoresis* **2003**, *24*, 1451−1457.
(7) Shadpour, H.; Soper, S. A. *Anal. Chem.* **2006**, *78*, 3519−3527.
(8) Kim, B. Y.; Yang, J.; Gong, M. J.; Flachsbart, B. R.; Shannon, M. A.; Bohn, P. W.; Sweedler, J. V. *Anal. Chem.* **2009**, *81*, 2715−2722.
(9) Ramsey, J. D.; Jacobson, S. C.; Culbertson, C. T.; Ramsey, J. M. *Anal. Chem.* **2003**, *75*, 3758−3764.
(10) Mellors, J. S.; Gorbounov, V.; Ramsey, R. S.; Ramsey, J. M. *Anal. Chem.* **2008**, *80*, 6881−6887.
(11) Chambers, A. G.; Mellors, J. S.; Henley, W. H.; Ramsey, J. M. *Anal. Chem.* **2011**, *83*, 842−849.
(12) Lewis, K. C.; Opiteck, G. J.; Jorgenson, J. W.; Sheeley, D. M. *J. Am. Soc. Mass Spectrom.* **1997**, *8*, 495−500.

(13) Bergstrom, S. K.; Samskog, J.; Markides, K. E. *Anal. Chem.* **2003**, *75*, 5461−5467.
(14) Bergstrom, S. K.; Dahlin, A. P.; Ramstrom, M.; Andersson, M.; Markides, K. E.; Bergquist, J. *Analyst* **2006**, *131*, 791−798.
(15) Bushey, M. M.; Jorgenson, J. W. *Anal. Chem.* **1990**, *62*, 978−984.
(16) Bushey, M. M.; Jorgenson, J. W. *J. Microcolumn Sep.* **1990**, *2*, 293−299.
(17) Hooker, T. F.; Jorgenson, J. W. *Anal. Chem.* **1997**, *69*, 4134−4142.
(18) Larmann, J. P.; Lemmo, A. V.; Moore, A. W.; Jorgenson, J. W. *Electrophoresis* **1993**, *14*, 439−447.
(19) Lemmo, A. V.; Jorgenson, J. W. *Anal. Chem.* **1993**, *65*, 1576−1581.
(20) Lemmo, A. V.; Jorgenson, J. W. *J. Chromatogr.* **1993**, *633*, 213−220.
(21) Moore, A. W.; Jorgenson, J. W. *Anal. Chem.* **1995**, *67*, 3448−3455.
(22) Moore, A. W.; Jorgenson, J. W. *Anal. Chem.* **1995**, *67*, 3456−3463.
(23) Moore, A. W.; Larmann, J. P.; Lemmo, A. V.; Jorgenson, J. W. *Methods Enzymol.* **1996**, *270*, 401−419.
(24) Dalpathado, D. S.; Desaire, H. *Analyst* **2008**, *133*, 731−738.
(25) Wagner-Rousset, E.; Bednarczyk, A.; Bussat, M. C.; Colas, O.; Corvaia, N.; Schaeffer, C.; Van Dorsselaer, A.; Beck, A. *J. Chromatogr., B: Anal. Technol. Biomed. Life Sci.* **2008**, *872*, 23−37.
(26) Bongers, J.; Devincentis, J.; Fu, J. M.; Huang, P. Q.; Kirkley, D. H.; Leister, K.; Liu, P. R.; Ludwig, R.; Rumney, K.; Tao, L.; Wu, W.; Russell, R. J. *J. Chromatogr., A* **2011**, *1218*, 8140−8149.
(27) Lim, A.; Reed-Bogan, A.; Harmon, B. J. *Anal. Biochem.* **2008**, *375*, 163−172.
(28) Griffiths, S. K.; Nilson, R. H. *Anal. Chem.* **2001**, *73*, 272−278.
(29) Jacobson, S. C.; Hergenroder, R.; Koutny, L. B.; Warmack, R. J.; Ramsey, J. M. *Anal. Chem.* **1994**, *66*, 1107−1113.
(30) Mellors, J. S.; Jorabchi, K.; Smith, L. M.; Ramsey, J. M. *Anal. Chem.* **2010**, *82*, 967−973.
(31) Krokhin, O. *Expert Rev. Proteomics* **2012**, *9*, 1−4.
(32) Moruz, L.; Tomazela, D.; Kall, L. *J. Proteome Res.* **2010**, *9*, 5209−5216.
(33) von Muhlen, C.; Marriott, P. J. *Anal. Bioanal. Chem.* **2011**, *401*, 2351−2360.
(34) Reichenbach, S. E.; Carr, P. W.; Stoll, D. R.; Tao, Q. P. *J. Chromatogr., A* **2009**, *1216*, 3458−3466.